

3D numerical modeling of rock cutting experiments under confining pressure through discrete element method

N. Gonze, F. Descamps & J-P. Tshibangu

University of Mons, Mons, Belgium

ABSTRACT: Understanding destruction mechanisms in high depth conditions is important to correctly manage the drilling of very-deep boreholes. Regarding Polycrystalline Diamond Compact drill bits, which dominate the drilling bits market, cutting mechanism is well known in atmospheric conditions but its understanding in a confining environment needs to be improved. In this research, we use a 3D Discrete Element method to study the influence of confining conditions and some cutting parameters on the Mechanical Specific Energy. With this approach, we highlight good correlation between numerical models and laboratory experiments performed on Single cutter machines. Considering the important cost and difficulties to drive experimental tests on these devices the elaborated numerical method could be an interesting alternative to go deeper in the understanding of cutting mechanism.

1 INTRODUCTION

The understanding of the destruction mechanisms in a confined environment is essential for optimizing deep drilling, not only for the gas and oil industry but also in the context of deep geothermal energy recovery or CO₂ storage. A thorough understanding of the evolution of these mechanisms with high depth conditions (confinement, temperature, etc.) will help making the most suitable choice of the tool and its design. This will also allow to use the drill bit in its optimal conditions: weight on bit, rounds per minute, rate of penetration, etc.

Arrived in the 70's on the market, the PDC (Polycrystalline Diamond Compact) bits never stopped to increase their market share and represent now 90% of the total distance drilled per year. Considering this domination of the PDC drill bits, it makes sense to study more closely the destruction mechanism involved by these drilling tools: the cutting mechanism.

Researches have already been conducted to understand this mechanism. Currently the cutting mechanism is well understood in atmospheric conditions that are in fact far away from the conditions in deep boreholes (confinement due to the drill mud and natural stresses, temperature,...). There is therefore still a lot of work to do on this specific aspect of the problem.

While research about the cutting mechanism in atmospheric conditions is largely based on laboratory tests, the same is not true when studying the effect of the confinement. Indeed, the developed laboratory facilities for this purpose, allowing to use one or more cutters at a time, are complex machines that are difficult and costly to operate. Moreover, it is not possible to modify many parameters and the measurements are not always easy to interpret.

Currently one solution to overcome this problem is the use of numerical models. The challenge is that the cutting process leads to the development of fractures and the creation of new contacts that can be better simulated by the Discrete Element Method.

In this paper, we use PFC3D to study the cutting mechanism in a confined environment. Firstly, we calibrated a synthetic rock model based on Vosges Sandstone mechanical properties; this choice is justified by the fact that this sandstone is one of the rock often used to study the rock cutting mechanism (Dagrain et al. 2001, Yahiaoui et al. 2016, Amri et al. 2016, Zhou & Lin 2014).

After this calibration and a validation of the model, we applied a full testing protocol to study the impact of several parameters on the destruction mechanism. These results are finally compared with single cutter experiments published in the literature to check the quality of our numerical model.

2 DISCRETE ELEMENT MODEL: CALIBRATION AND VALIDATION

2.1 *Discrete element method*

The Discrete Element Method used in this work is a subcategory of the Distinct Element Method developed by Cundall (1971) to analyze fractured rock mass. The Discrete method was initially developed by Cundall & Strack (1979) to study the non-cohesive media. It was later adapted for the study of cohesive materials by taking into account the granular micro-texture of the rock.

In the Discrete Element Method applied on rocks, the material is represented as an assembly of bonded rigid particles (spheres in 3D) interacting together at their contact points. The bonds between particles are generally defined by tensile and shear strengths, normal and tangential stiffnesses as well as a friction coefficient. All these parameters are called micro-properties.

Among the different bond models, we applied the specific parallel one for which micro-properties can be viewed as the physical representation of the cement between particles. For more details on the Bonded Particles Method refer to Potyondy & Cundall (2004).

When the model is subjected to external forces, the stresses between particles can exceed the bond strength, which generates bond failures and creates cracks. The propagation of the cracks can be easily tracked in DEM without needing additional numerical treatment.

2.2 *Model calibration*

As explained before, the behavior of the synthetic rock is governed by micro-properties defining interactions between model particles. These microproperties are not directly linked to the mechanical properties of the material (UCS, Young's modulus, Poisson's ratio) and hence need to be fixed following a calibration procedure. The general calibration method proposed by Potyondy & Cundall (2004) and Itasca Consulting Group (2008) is based on an iterative procedure simulating an uniaxial test. The goal is to adjust iteratively several micro-properties until the behavior and macro-properties obtained in the model are the same as the ones observed for the real rock.

Considering that this study is conducted in a confined environment, we added a triaxial test in the calibration procedure to reproduce the behavior of the rock under confinement. The data used to calibrate the Vosges sandstone synthetic model are from Tshibangu & Descamps (2012).

Figure 1(A) shows the comparison between the triaxial test carried out in the laboratory at 20 MPa of confining pressure and the one obtained at the end of the calibration process. The set of parameters reproducing the behavior of the Vosges sandstone as accurately as possible is listed in Table 1.

Table 1. Micro-properties used to simulate Vosges sandstone.

Micro-properties	Values
Minimum ball radius (mm)	0.1
Ball size ratio	3
Contact modulus (GPa)	4
Ball stiffness ratio	8
Ball friction coefficient	0.3
Parallel bond modulus (GPa)	4
Parallel bond stiffness ratio	0.2
Parallel bond tensile strength (MPa)	200 ± 20
Parallel bond shear strength (MPa)	200 ± 40

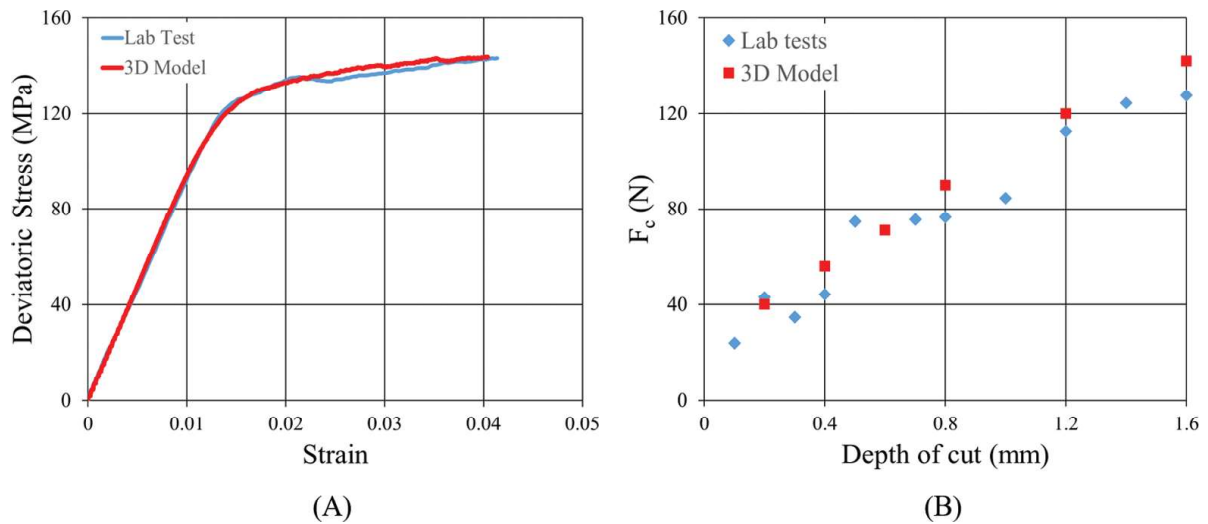


Figure 1. Results of the calibration and validation steps: (A) Comparison between experimental and numerical triaxial tests at 20 MPa of confinement; (B) Comparison between mean cutting forces measured in laboratory on a Rock Strength Device and the ones obtained with the numerical model after calibration in the same atmospheric conditions.

2.3 Model validation

Before going deeper into the problem of cutting under confinement, the model was validated from a cutting mechanism point of view. For this, tests were performed on a Rock Strength Device (RSD). This device is dedicated to linear cutting tests in atmospheric conditions (Richard et al. 2012).

We simulated cutting tests at different depths of cut and compared them with the tests performed on the RSD. Figure 1(B) compares the laboratory results with the numerical ones. The cutting forces obtained with the model at different depths of cut are in a good agreement with the ones measured in the lab.

3 TESTING PROTOCOL

3.1 Description of the cutting model

The cutting simulation implemented in this work is the linear displacement of a circular sharp PDC cutter along the rock specimen with constant velocity and depth of cut. The sketches in Figure 2 illustrate the general geometry and the cutting parameters.

Regarding the synthetic rock sample, the dimensions H , L and W remained the same for all models and were respectively 8 mm, 25 mm and 20 mm. It should also be noted that the same sample was used for all the models. The use of the same sample avoids the discussion about the arrangement of grains (even though this impact is very small).

Another feature was implemented to reduce the calculation time. Indeed, we used a refinement function to have different grain size distributions in the model (Itasca Consulting Group, 2008). Only the zone affected by the cutting mechanism were modeled with the ball size distribution used in the calibration. Below a depth of 3 mm, larger size particles were used in order to reduce the number of elements and therefore the calculation time.

For the cutting parameters, some of them were kept constant for all the numerical analyses:

- \varnothing : cutter diameter = 13mm
- BR: back rake angle = 15°
- CT: cutter thickness = 8mm

Figure 3(A), gives a 3D view of the complete DEM model used in this work.

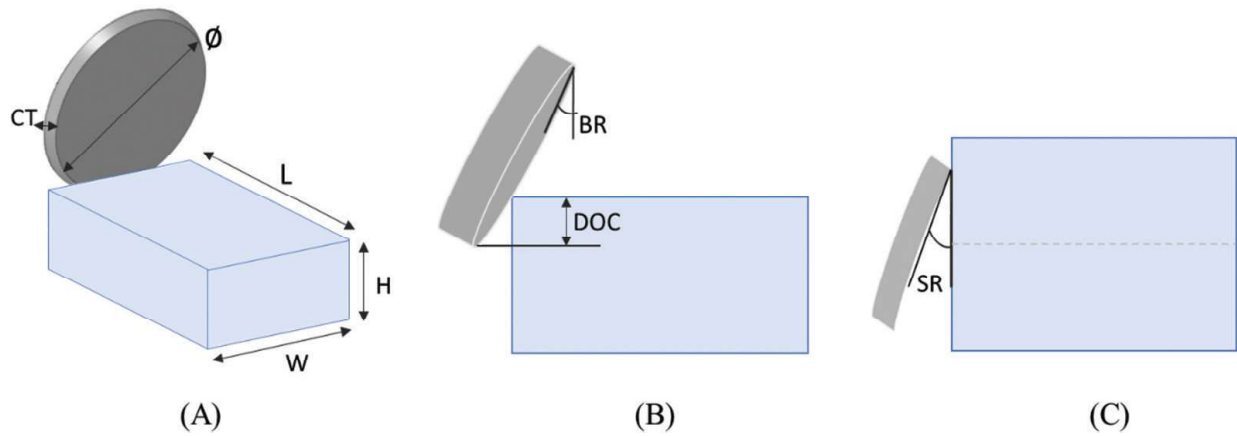


Figure 2. Schematic views of the model: (A) 3D view; (B) lateral view, (C) top view. [L = sample length; H = sample high; W = sample width; CT = cutter thickness; ϕ = cutter diameter; DOC = depth of cut; BR = back rake angle; SR = side rake angle]

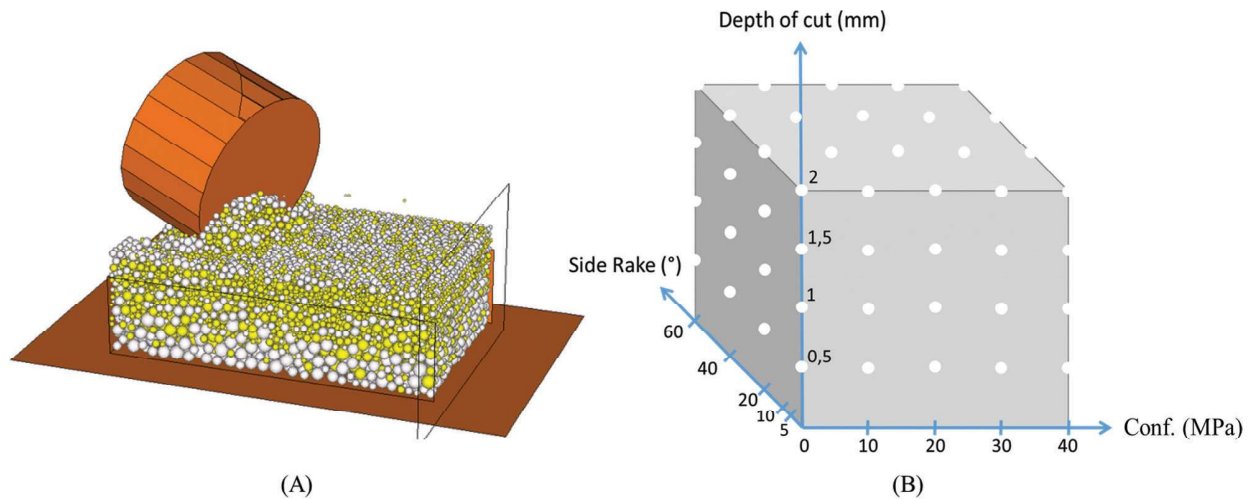


Figure 3. (A) 3D view of the numerical model; (B) Full factorial design of simulations implemented in this work.

3.2 Test plan

Finally, among all the parameters, the work for this research was focused on the impact of three parameters: the depth of cut (DOC), the side rake angle (SR) and the confining pressure. With those three independent variables, a full factorial design of simulation was created with a total of 120 sets of parameters. Figure 3(B) gives a graphical representation of the full factorial design with the values tested for each parameter. The cutter speed was fixed to 1 m/s for all the tests.

The outputs registered during the simulations were the forces acting on the face of the cutter: the cutting force, the thrust force and the lateral one, which will be respectively represented in red, green and blue in the following plots.

4 RESULTS AND DISCUSSION

Figure 4 presents the evolution of the forces during a test at a depth of cut of 1 mm, a confinement of 20 MPa and a side rake angle of 0° . We can observe two parts in the evolution of the forces. First, we have a transitional phase from 0 to 1 cm. This transitional phase is the distance needed for the cutter to be fully into contact with the rock sample and to allow the formation of a crushed ribbon (Kaitkay & Lei 2005). After this first phase, the forces reach a steady state with a slight increase during the tests.

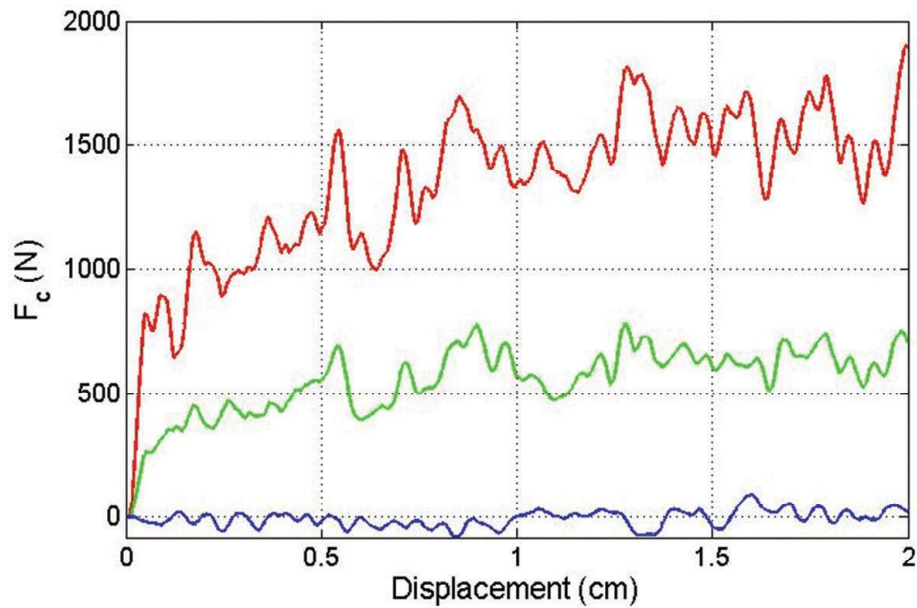


Figure 4. Evolution of the cutting forces during a simulation at 20 MPa of confining pressure and a Side Rake of 0° (Red = cutting force, Green = thrust force, Blue = lateral force).

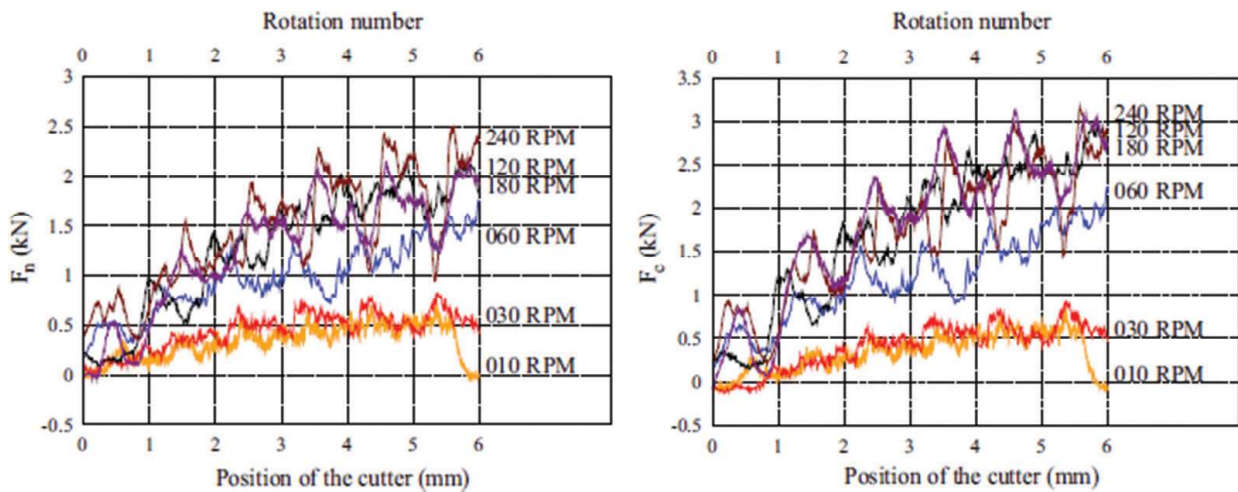


Figure 5. Variation of the cutting forces with the vertical position of the cutter at 20 MPa on the Vosges Sandstone at DOC of 1 mm; on the left, thrust force and on the right, cutting force (Amri et al. 2016).

One of the features of our codes can explain this steady state. Indeed, we limit the amount of crushed material that can accumulate in front of the cutter. The thickness of this accumulation was limited to twice the depth of cut.

Compared to the results published in the literature (Amri et al. 2016) and shown in Figure 5, cutting forces obtained in the model are in the same range as the ones observed in laboratory experiments. In contrast, thrust forces appear to be underestimated. This underestimation can be justified by two important differences between the numerical model and the laboratory tests.

First, the modeled tool in this work is a perfectly sharp and rigid tool that cannot wear out. However, in practice, the tools used for laboratory studies are generally chamfered tools that can be blunt or present a wear flat due to the previous experiments. Moreover, the presence of a chamfer and a wear flat has a significant impact on the thrust force (Rostamsowlat et al. 2018).

Secondly, the methodology used in the model could explain the underestimation of the thrust force. Indeed, the numerical model imposes a constant depth of cut while the laboratory experiments impose a constant rate of penetration. This constant rate of penetration could need more vertical force to continuously increase the depth of cut.

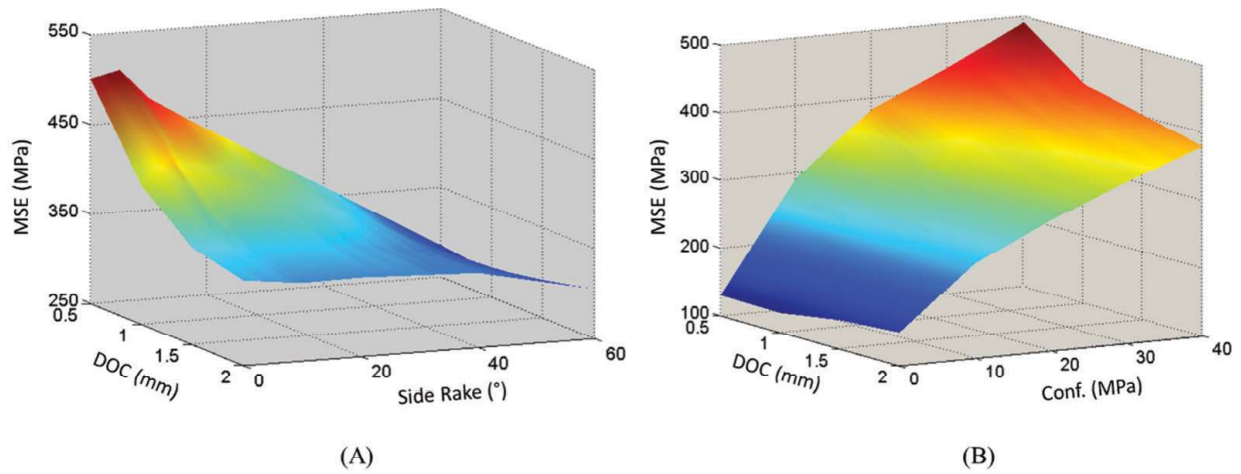


Figure 6. Mapping of the MSE; (A) Mapping for a confining pressure of 30 MPa, (B) Mapping for a Side Rake of 20°.

More than forces, it is interesting to look at another parameter commonly used to measure cutting efficiency: the mechanical specific energy (MSE) developed by Detournay & Defourny (1992). This parameter is defined as the energy needed to excavate a unit volume and it is evaluated as following:

$$MSE = \frac{F_c}{A_c} \quad (1)$$

where F_c = average cutting force during the steady state phase; A_c = cross-section of the groove and MSE unit is MPa.

With the help of the full factorial design implemented, it was possible to map the MSE for different cutting conditions (Figure 6).

Based on the mappings on Figure 6, it should be noted that the MSE tends to decrease when the depth of cut increases. Akbari & Miska (2016) who performed cutting tests at different confining pressures and depths of cut on a single cutter machine observed the same trend.

Regarding the side rake angle, it seems to have a bigger impact at small depth of cut than at high depth. Indeed, Figure 6(A) shows an strong decrease of the MSE for a depth of cut of 0.5 mm. Conversely, in the case of a depth of cut of 2 mm, the side rake has almost no influence. These observations still need to be validated by rotational cutting models that will be more consistent with the reality.

5 CONCLUSIONS AND OUTLOOKS

The purpose of this work was to study the cutting mechanism by 3D DEM numerical simulation to see if this modeling technique could be a cost effective complement to the tests on single cutter machines.

Our simulations are in good agreement with our laboratory tests in atmospheric conditions on a Rock Strength Device. They also follow the same trends as the ones published in the literature in terms of cutting forces and MSE evolution with the depth of cut or the side rake in the case of tests made in a confined environment.

Considering all the simulations, it was possible to map the evolution of the MSE versus several parameters. These mappings could be good tools to find the best cutting parameters to choose in order to reduce the MSE considering an imposed parameter (targeted rate of penetration, confining pressure, etc).

The current drawback of the DEM model is the underestimation of the thrust force. This underestimation could be easily corrected by implementing in the model chamfered cutters or blunt cutters. From this interesting base, improvements can still be made to get closer to reality.

The first improvement should be the simulation of rotational cutting test with a constant rate of penetration allowing the overlap of multiple grooves. This would ensure that the model does not only provide cutting forces of the same order of magnitude as those measured in laboratories but also allow having the same forces evolution considering successive cuts in the same groove.

The second important evolution deals with modeling of the material behavior by firstly taking into account the effect of the pore pressure.

Finally, it would be very interesting to be able to implement into the model the evolution of the constitutive law of the rock, due to the high depth conditions. It would then be possible to link the constitutive behavior with the mechanical specific energy or, more globally, the cutting mechanism.

REFERENCES

- Akbari, B. & Miska, S. 2016. The effects of chamfer and back rake angle on PDC cutters friction. *Journal of Natural Gas Science and Engineering* 35: 347–353.
- Amri, M., Pelfrene, G., Gerbaud, L., Sellami, H. & Tijani, M. 2016. Experimental investigations of rate effects on drilling forces under bottomhole pressure. *Journal of Petroleum Science and Engineering* 147: 585–592.
- Cundall, P.A. 1971. A computer model for simulating progressive, large-scale movements in blocky rock systems. In *Proc. Symp. Int. Rock Mech.* Nancy.
- Cundall, P.A. & Strack, O.D.L. 1979. A discrete numerical model for granular assemblies. *Géotechnique* 29(1): 47–65.
- Dagrain, F., Detournay, E. & Richard, T. 2001. Influence of Cutter Geometry in Rock Cutting. In *In DC Rocks 2001, The 38th US Symposium on Rock Mechanics (USRMS)*. American Rock Mechanics Association.
- Detournay, E. & Defourny, P. 1992. A phenomenological model for the drilling action of drag bits. *International Journal of Rock Mechanics and Mining Sciences* 29(1): 13–23.
- Itasca Consulting Group. 2008. PFC3D – Particle Flow Code in 3 Dimensions, Ver. 4.0 User's Manual.
- Kaitkay, P. & Lei, S. 2005. Experimental study of rock cutting under external hydrostatic pressure. *Journal of Materials Processing Technology* 159(April 2004): 206–213.
- Potyondy, D.O. & Cundall, P. a. 2004. A bonded-particle model for rock. *International Journal of Rock Mechanics and Mining Sciences* 41: 1329–1364.
- Richard, T., Dagrain, F., Poyol, E. & Detournay, E. 2012. Rock strength determination from scratch tests. *Engineering Geology* 147–148 (August):91–100.
- Rostamsowlat, I., Richard, T. & Evans, B. 2018. An experimental study of the effect of back rake angle in rock cutting. *International Journal of Rock Mechanics and Mining Sciences* 107(April): 224–232.
- Tshibangu, J.-P. & Descamps, F. 2012. The FPMs (UMons-Belgium) device for investigating the mechanical behavior of materials subjected to true triaxial compression. In *True Triaxial Testing of Rocks*. Geomechanics Research Series. CRC Press, 51–60.
- Yahiaoui, M., Paris, J.Y., Delbé, K., Denape, J., Gerbaud, L. & Dourfaye, A. 2016. Independent analyses of cutting and friction forces applied on a single polycrystalline diamond compact cutter. *International Journal of Rock Mechanics and Mining Sciences* 85: 20–26.
- Zhou, Y. & Lin, J.S. 2014. Modeling the ductile-brittle failure mode transition in rock cutting. *Engineering Fracture Mechanics* 127: 135–147.